Semiconductor Optoelectronics, *Vol. 42 No. 1 (2023), 1234-1255*
https://bdtgd.cn/

CHARACTERIZATION OF SILICON RUBBER DOPED WITH BISMUTH (III) OXIDE (Bi_2O_3) AND BORON NITRIDE (hBN) FOR NEUTRON AND GAMMA RADIATION SHIELDING COMPETENCES VIA GEANT4-TOOLKIT AND PY-MLBUF

Amit Joshi[a,*], Genius Walia[a], Kulwinder Singh Mann[b]

[a]Department of Physics, Guru-Kashi University, Talwandi-Sabo, Punjab, India
[b]Department of Physics, D.A.V College, Bathinda-151001, Punjab, India

ABSTRACT

The neutron-gamma shielding behavior (NGSB) of silicon rubber matrix amalgamated with bismuth (III) oxide (Bi_2O_3) and hexagonal boron nitride (hBN) was studied in energy range 1-10 MeV based on different shielding parameters *viz.* mass attenuation coefficient (*MAC*), equivalent atomic number (Z_{eq}), exposure buildup factor (*BUF*), mass effective removal cross-section (*MERC*), half-value layer (*HVL*), and tenth value layer (*TVL*) thickness. The Monte-Carlo simulation-based GEANT4 toolkit and Geometrical-Progression fitting plus American Standards (ANS/ANSI-6.4.3) based online platform, Py-MLBUF were used. *MAC* values computed by GEANT4 and Py-MLBUF showed a reasonable agreement (r=0.99) and relative difference between the two was not significant (α=0.05), confirming the deviations in values calculated from GEANT4 and Py-MLBUF were acceptable. The results were statistically analyzed using two-way analysis of variance (ANOVA) and indicated significant impact of sample composition and incident energy on NGSB. An increase of 30% Bi_2O_3 by wt. in SRB3 increased its *MAC*, Z_{eq} and decreased the *HVL* and *TVL* values, implicating higher level of Bi_2O_3 in the composite sample (SRB3) enhanced its gamma-ray shielding capability. The presence of low-Z elements in SRB1 improved its *MERC* value in the selected energy range and indicated SRB1 a good alternative for conventional neutron shielding materials. Therefore, the amalgamated silicon rubber matrices, SRB1 and SRB3, were found to be the potential fast neutron and gamma radiation attenuator, respectively in energy range 1-10 MeV. This study would be useful for prospective utilization of doped silicone rubber as effective neutron- gamma shielding material in advanced nuclear radiation technology.

Keywords: Neutron, Gamma ray, Shielding, Silicon Rubber, GEANT4, Py-MLBUF

1. Introduction

Human exposure to ionising radiation can be due to natural (cosmic rays radiating from soil or rock) or man-made (x-ray generators, medical devices and nuclear reactors) sources (K S Mann et al. 2012). These high-energy neutron and gamma radiation interact with the tissues

* Corresponding author: Amit Joshi, Department of Physics, Guru-Kashi University, Talwandi-Sabo, Punjab, India.
E-mail address: dheerajjoshi96@gmail.com

and organs and beyond certain thresholds can cause cell mutations, skin burns, cancerous growths, acute radiation sickness and death. Different factors such as dosage and type of radiation and the sensitivity of the tissues and organs determine the severity of the harm caused. Though these ionizing radiations have found economic importance in large array of significant applications spanning nuclear medicine, business, agriculture, and research, it is crucial to carefully evaluate the potential generation of free radicals at various energies that may impair the biological cells (Ambika et al. 2017; Bagheri, Khorrami Moghaddam, and Yousefnia 2017; Al-Hadeethi and Sayyed 2020). Along with rapidly growing demand for ionizing radiations, the health hazards may also increase unless these radiations are utilized properly and effective shielding is used to curb the radiation exposure (Al-Hadeethi, Sayyed, and Nune 2021).

To design a suitable radiation shield it is necessary to understand the attenuation properties of the shielding materials. A broad range of materials such as building block materials, concrete, steel, polymers, clay, composites, paraffin, resins, and alloys have been studied in past for their radiation shielding potential (Singh and Badiger 2014; Biswas et al. 2016; Harrison et al. 2008; Mollah, Ahmad, and Husain 1992; Mann K.S et al. 2013; Olukotun et al. 2019; Mirji and Lobo 2017). The shielding behavior of a material can be determined from its effective removal cross-section (*ERC*, cm^{-1}) and attenuation coefficient (μ, cm^{-1}) along with its optical thickness (*OT*, mfp) (Olukotun et al. 2019; Mann et al. 2013). The build-up factor (*BUF*) measures the contribution of the scattered radiation and plays an important role in studying neutron-gamma shielding behavior (NGSB) (V P. Singh and Badiger 2012; Amirabadi et al. 2013). The photon attenuation varies with the atomic number (Z), thickness and mass density of the material (Içelli et al. 2013; Mann et al. 2013; Singh and Badiger 2012). Therefore, elements with higher atomic number (Z) such as bismuth and lead are highly effective for gamma shielding whereas the low Z and high density materials such as water, wood, paraffin are recommended for neutron shielding in the past (Ahmed et al. 2020; Erdem et al. 2010). Thus, both heavy and light elements should be considered to make a composite or mixture capable of attenuating both neutrons and gamma rays. While selection, elements exhibiting higher energy loss per collision, and high absorption cross-section with no secondary gamma ray emission should be considered. Rubber is a cost effective and promising material for gamma and neutron radiation shielding which can be assembled into variety of shapes and size without altering their composition and density by external fields (El-kameesy et al. 2017; Intom et al. 2020).Silicon rubber is resistant to ozone, ultraviolet light, and extreme heat in different environments and widely used in adhesives, electronics, electrical network systems and medical applications (Shit and Shah 2013). In addition, it is soft, stable, non-combustible and non-toxic and can be utilized for radiation shielding applications. Filler incorporation can be used to tailor its low-elasticity and tensile value (Özdemir and Yılmaz 2018). Bismuth oxide and Boron compounds were used as functional filler materials in the polymeric matrix and were renowned for their gamma and neutron absorption ability (Park et al. 2015). The present investigation aims to study the neutron and gamma shielding behavior of flexible composites based on a silicone rubber matrix amalgamated with bismuth (III) oxide (Bi_2O_3) and hexagonal boron nitride (hBN) developed by Yilmaz *et al*. (Seda Nur Yılmaz, İsmail Kutlugün Akbay 2020).The neutron gamma shielding parameters of different silicon rubber composite materials was measured in the energy range 1-10 MeV with standard toolkits, GEANT4 (Agostinelli et al. 2003) and Py-MLBUF (K.S Mann and Mann 2021).

2. Theoretical background

2.1 Shielding parameters for Gamma rays

2.1.1 Linear Attenuation Coefficients (*LAC*, cm^{-1})

The probability of gamma rays interaction with matter through photo-electric absorption, Compton scattering and pair production depends on atomic number (Z) of target material and incident energy (E) of radiation. The linear attenuation coefficient (*LAC*) is the sum of all interaction probabilities that determines the material's effectiveness in gamma rays shielding. Radiation intensity reduction by shielding material follows the Beer Lambert law (K S Mann et al. 2012) $I=I_0e^{-\mu x}$ where I and I_0 refers to radiation intensities with and without shielding material respectively, x denotes the thickness of shielding material and μ is the *LAC* (Chang et al. 2015).

2.1.2 Mass Attenuation Coefficient (*MAC*, $cm^2\ g^{-1}$)

The mass attenuation coefficient (*MAC*) accounts for the material compaction effect on its shielding performance measuring all types of interaction probabilities of gamma photon and shielding material occurring in the area l thickness ($X_m=\rho.x$) of the material. *MAC* (μ_m) is calculated from $I = I_o e^{-\mu x X_m}$. *MAC* (μ_m) is also obtained by division of *LAC* (μ) with mass density (ρ), *MAC* (μ_m) = *LAC* (μ)/ ρ

2.1.3 Half-Value Layer (*HVL*, cm) and Tenth Value Layer (*TVL*, cm)

The half-value layer (*HVL*) defines the thickness of shielding material which attenuates the gamma rays intensity to half and quantifies how efficiently a substance can shield gamma rays. Similarly, the tenth value layer (*TVL*) is the material thickness that attenuates gamma rays intensity to 10% of the incident intensity. Thus, *TVL* is always greater than *HVL* (*TVL* >*HVL*). Mathematically,

$$HVL = \frac{\ln 2}{\mu} = \frac{0.693}{\mu} = 0.693\,mfp$$

$$TVL = \frac{\ln 10}{\mu} = \frac{2.3026}{\mu} = 2.3026\,mfp$$

2.2 Shielding parameters for Neutrons

2.2.1 Effective Removal Cross-sections (*ERC*, cm^{-1})

For an incident fast neutron, the microscopic cross-section (σ, cm^2) of the shielding material measures its probability of interaction (scattering/absorption) with the nucleus of shielding element. On the other hand, the total macroscopic cross-section (Σ_t) or effective removal cross-section (*ERC*) provides the effective area of all the nuclei of the shielding material that interact with the traversing neutron (Rinard 1990). Mathematically,

$$\sum_t = \sigma_t \left(\rho . N_a / A \right)$$

where N_a denotes Avogadro's number, σ_t is total microscopic cross-section (cm^2), ρ denotes the density (g cm^{-3}) and A is the effective atomic mass of shielding material. The neutron attenuation in medium also follows the Beer Lambert law (Rinard 1990)

$$N = N_o \exp\left(-\sum_t .T\right)$$

where N_o and N are incident and transmitted flux of neutrons respectively for the shielding material of thickness, T (cm).

2.2.2 Mass Effective Removal Cross-section (*MERC*, $cm^2\ g^{-1}$)

The mass effective removal cross-section (*MERC*) obtained from *ERC* and mass density (ρ) of the shielding material was introduced to consider the material's compaction effect on its shielding behavior. The *MERC* of a shielding material for the fast neutrons (8 MeV) is estimated with following empirical formulae (Wood 1982):

For A>10 and A <12: $MERC_1 = 0.21.A^{-0.56} cm^2 g^{-1}$

For A >12: $MERC_2 = 0.00662.A^{-1/3} + 0.33.A^{-2/3} - 0.211.A^{-1} cm^2 g^{-1}$

For $Z \leq 8$: $MERC_3 = 0.190.Z^{-0.743} cm^2 g^{-1}$

where, Z denotes effective atomic number and A denotes effective atomic mass of the sample.

3. Materials and Methodology

The neutron gamma shielding behavior (NGSB) of silicon rubber composite materials was investigated for energy ranges of 1-10 MeV. The silicon rubber matrix amalgamated with hexagonal boron nitride (hBN) and bismuth (III) oxide (Bi_2O_3) functional fillers were developed by Yılmaz *et al* (Seda Nur Yılmaz, İsmail Kutlugün Akbay 2020). The elemental composition and details of four samples selected for study are given in Table 1. The neutron shielding parameters such as mass effective removal cross-section (*MERC)*, half-value layer (*HVL*) and tenth value layer (*TVL*), partial hadron elastic cross section (*PHEC*), neutron capture cross section (*NCCS*), neutron inelastic cross section (*NICS*), and mean free path (λ) of the selected samples were investigated using the GEANT4 toolkit based on Monte-Carlo simulation (Agostinelli et al. 2003). The gamma shielding parameters viz., mass attenuation coefficient (*MAC)*, half-value layer (*HVL*) and tenth value layer (*TVL*), buildup factor (*BUF*) and gamma transmission flux were analyzed using GEANT4 and Py-MLBUF online platform (K.S Mann and Mann 2021).

3.1 GEANT4 toolkit

GEANT4 is geometry and tracking computer code developed by CERN for simulating particle passage through matter using experimental particle reaction cross-sections (Agostinelli et al. 2003). Using theoretical and experimental advancements in electromagnetic and hadronic processes, GEANT4 can track particles to zero energy ranges. In this simulation work, GEANT4 version 4.10.04 was used in which low-energy (thermal to 20 MeV) neutron interactions cross-section data were taken from ENDF/B- VI (Rose P.F 1991). GEANT4 electromagnetic processes were used to investigate the gamma-ray shielding by silicone rubber composite materials. Initially, the elemental composition and mass density of the sample is required. After designing the experimental geometry, the simulation can be initialized by setting the number of incident particles as shown in Fig. 1.

3.2 Py-MLBUF-Online platform

Python program for Multi-Layered Buildup Factors (Py-MLBUF) is an open-access, user-friendly, and fastest among similar online platforms (BXCOM and Phy- X/PSD),

calculate 36 gamma ray shielding (GSP) parameters in energy range 0.015 to 15 MeV and provides graphical representation of results.

3.3 Validation of GEANT4 and Py-MLBUF

For gamma shielding, GEANT4 and Py-MLBUF results for standard materials, iron and water were compared with previously published XCOM, ANS-standard and MCNP5 results (L. Durani 2009). The ratios of calculated mass attenuation coefficients to respective standard values in the selected energy range of 1-10 MeV were found close to 1 Fig. 2(a-b), advocating the precision of GEANT4 and Py-MLBUF.

For neutron shielding, the accuracy of GEANT4 simulation was ensured by comparing the computed values of effective removal cross-sections (*ERC*) with experimental values for different concrete samples selected as reference from earlier research works (Mollah, Ahmad, and Husain 1992; Bashter, Makarious, and Abdo 1996; Gallego, Lorente, and Vega-Carrillo 2009). Reasonable agreement was found between *ERC* values calculated with Geant 4 and reference data, providing confidence in the findings of GEANT regarding neutron attenuation of doped silicon rubber.

3.4 Statistical Analysis

A two-factor analysis of variance (ANOVA) was conducted to investigate the response of selected samples to NGSP (*MAC* and *MERC*) at different energies using OP stat software. The variance of expression among the samples (S) at different energies (E) and interaction between samples and energy (S x E) was studied. The mean performance of the samples for *MAC* and *MERC* was also studied to identify the best composition for effective shielding against neutrons and gamma rays. The association among the *MAC* values calculated from GEANT4 and Py-MLBUF was estimated through correlation coefficient using MS Excel. The two softwares were compared based on *MAC* values using t test in MS Excel.

4. Results and discussion

The NGSB of the selected samples was investigated by analyzing the gamma and neutron shielding parameters computed using the standardized toolkits.

4.1. Gamma radiation shielding parameters

Mass Attenuation Coefficient (*MAC*, $mm^2 g^{-1}$)

The *MAC* values for all the samples were calculated with the Py-MLBUF and GEANT4. The variation in three partial photon interaction coefficients, viz., photoelectric absorption attenuation coefficient (*PEAC*), Compton scattering attenuation coefficient (*CSAC*), and pair-production attenuation coefficient (*PPAC*) along with their combined effect (*MAC*) for the selected samples with energy are represented in Fig. 3(a-d). *MAC* values for all the samples were higher in photoelectric region and reduced gradually in Compton scattering region. Above 4MeV, the pair production dominates causing varied response of samples with respect to mass attenuation coefficient (Fig. 4). The *MAC* values (mm^2g^{-1}) in energy range 1-10MeV was found highest in SRB3 (6.842 to 2.978 followed by SRB2 (6.770 to 2.689), SRB4 (6.698 to 2.40) and SRB1 (6.918 to 2.251). The highest *MAC* value in SRB3 can be due to the presenceof high Z element, Bi (26.91% by wt) which makes SRB3 the most effective shielding material for gamma ray attenuation among the samples under study. In the low energy region, mass attenuation coefficient is observed to be maximum, because of dominant photoelectric

interaction which depends on atomic number as $Z^{(4-5)}$. In the intermediate energy region, Compton scattering becomes dominant which depends linearly with atomic number. Hence, mass attenuation coefficient values become minimum. In the high energy region, mass attenuation coefficient values again increase because of pair production which is proportional to Z^2 (V. P. Singh and Badiger 2014). As the percentage of bismuth (III) oxide (Bi_2O_3) increased from 0% (SRB1) to 30% (SRB3) (Table 1), the *MAC* value increased from 2.251 to 6.84mm^2g^{-1} (Fig. 4), indicating *MAC* value is the function of energy and chemical composition of the shielding material (Bashter 1997; Luis Durani 2009; H. Singh et al. 2016). Furthermore, *MAC* values computed by GEANT 4 and Py-MLBUF showed a reasonable agreement (r=0.99) and the relative difference between the two was not significant (α=0.05), confirming the deviations in values calculated from GEANT 4 and Py-MLBUF are acceptable (Table 3).

Half-Value Layer (*HVL*, cm) and Tenth Value Layer (*TVL*, cm) thickness

HVL and *TVL* represent the depth to which a radiation of specific energy could penetrate the material. Lower value portrays the better shielding potential of material (Sadawy and El Shazly 2019; Aygün 2019). In silicon doped rubber samples under study, *HVL* ranged from 10.415 to 31.689cm (Fig.5). It increased as the energy goes up from 1MeV to 10 MeV, suggesting that growing energy of photons enable them to pointedly penetrate the silicon rubber samples. *HVL* was found highest in SRB1 (31.68cm) and lowest in SRB3 (24.50cm) at 10MeV. The respective increase of boron nitride and bismuth (III) oxide from 0 to 10% and 30% in SRB3 reduced its *HVL*, thereby increasing its efficacy in shielding the radiations and making it the best attenuator in this study. Conversely, SRB1 with the largest *HVL* was the worst attenuator. The *TVL* ranged from 34.596 to 105.269cm in the selected samples (Fig. 6). The trend for *HVL* and *TVL* was similar, minimal at low energy level and increased progressively with increase in energy. At low energy, all the samples showed almost similar value. In intermediate to high-energy regions, the chemical composition significantly affects these parameters. The higher (30%) content of bismuth (III) oxide (Bi_2O_3) in SRB3 reduced the penetration level of radiation leading to minimum value of *TVL*. Thus, SRB3 possess the superior gamma radiation shielding properties as compared to the other samples. Composition of shielding material being an important factor for shielding high energy radiations was also reported in the past (Içelli et al. 2013; Aşkın 2019; K. S Mann et al. 2013; N. Singh et al. 2004).

Buildup factor (*BUF*)

The *BUF* values of the silicone rubber composite materials increased with penetration depths (Fig. 7a–h). The variations in *BUF* values for all selected materials were identical up to gamma energy of 3 MeV. In low energy regions (<2 MeV), the composite with the lowest value of Z_{eq} (SRB1) showed the highest *BUF* values whereas the composite with the highest Z_{eq} (SRB3) has relatively small *BUF* values (Fig.8). Therefore, in low energy regions the *BUF* depends upon the chemical composition. This illustrates that, the Lambert Beer's law violated minimally at low incident energies even for the high penetration depth of 40 mfp. It shows that in the low energy regions, the photoelectric effect is dominant process over Compton scattering. For incident photon energy of 2 MeV (Fig. 7b), *BUF* becomes almost independent of chemical composition (i.e. Z_{eq}) and its magnitude decreases. However, Compton scattering multiplicity has increased and the interacting material cannot even be recognized. In high

energy region (>3 MeV) pair production dominates the Compton scattering process, lowering *BUF* values. Electron–positron pair particles may enable more Compton scattering targets in the high-energy region. The electron–positron pair particles have a chance to escape from the medium with low penetration depths, but they scatter at high penetration depths and generate secondary gamma-ray photons by annihilating the positron with the electron at rest to increase photon intensities. At high incident energy (Fig. 7d-h) and for penetration depth greater than 10mfp, SRB3 (maximum Z_{eq}) was observed to possess maximum *BUF* values, whereas SRB1 (minimum Z_{eq}) possess minimum *BUF* values. The reversal in trend can be explained by the fact that pair production is the dominant process for this incident photon energy (V P. Singh, Badiger, and El-Khayatt 2014).

Gamma transmission flux

The gamma transmission flux is the ratio of the radiation intensity (I) with the shielding material present to the radiation intensity (I_0) without shielding material. Fig. 9 illustrates the variation in the gamma-ray intensity of silicone rubber composite materials with energies and shows that transmission flux increases with increasing energy. It was found that the attenuation coefficient depends on the incident photon energy as well as the chemical composition of the samples. The maximum transmission flux for SRB1 was due to the presence of low-Z elements, while SRB3 contains a high Z element (Bi; Z = 83, fractional weight = 0.269) which transmits a much lower fraction of incident gamma-ray, leads to a reduction of the transmission flux.

4.2. Neutron shielding parameters

In analogy to *MAC*, the *MERC* value also represents the combined effect of three partial neutron interaction processes, viz. partial hadron elastic cross section (*PHEC*), neutron capture cross section (*NCCS*), and neutron inelastic cross section (*NICS*). Fig. 10 (a-d) represents the variation of all the cross sections for the selected samples with neutron energy. The variation in *MERC* with photon energy indicates that the *MERC* values decrease with an increase in photon energy (Fig. 11). SRB1 has the maximum *MERC* values ranging from 36.52 to 9.33mm^2g^{-1}, while minimum *MERC* values are observed for SRB3, ranges from 24.10 to 6.87mm^2g^{-1} in the selected energy range. Higher the *MERC* of materials, the better the effectiveness in attenuating the traversing neutron beams (El-Khayatt 2010; Tellili, Elmahroug, and Souga 2014). This is due to the difference in chemical composition of the samples. SRB1 has a higher percentage of low Z elements by weight such as H (8.48%), C (36.08%) and O (21.62%), while SRB3 has a higher percentage of high Z element (Bi 26.91%). The interaction probability of neutrons depends on the atomic number (Z) of the constituent elements, the composition of the target material, and the incident energy (Bashter 2006; 1997). The ascending order of *HVL(N)* and *TVL(N)* is SRB1< SRB4 < SRB2 < SRB3. However, the *HVL(N)* and *TVL(N)* values increase with increasing energy (Figs 12 and 13). The dependence of *HVL(N)* and *TVL(N)* on the chemical composition of the materials can be clearly observed such that SRB1, comprising low-Z elements, had the lowest value and SRB3, comprising high-Z elements, had the highest values of *HVL(N)* and *TVL(N)*. Lower the values of *HVL(N)* and *TVL(N)*, greater the shielding efficacy of the material (Sadawy and El Shazly 2019; Aygün 2019). It has been concluded that SRB1 offers the highest shielding for the neutrons

4.3. Statistical Analysis

A comparison of variance components, samples (S), Energy levels (E) and S x E for

NGSP (*MAC* and *MERC*) exhibited their contribution to the total variance. Variance component for E was the largest for both the parameters (*MAC* and *MERC*) under study indicating the significant effect of energy level on the behavior of samples towards NGSB (Table 4). The sample was found to be significant, suggesting that the samples invariably responded differently among each other w.r.t the parameters studied. There was a significant contribution of S x E interaction variance on the sample expression for the parameters under study, indicating an interaction effect of the energy in relation to sample performance. The descriptive statistics of the samples under study are given in Table 5, indicates the behavior of samples in response to gamma rays and neutron rays based on their mean performance. The mean *MAC* value for SRB3 is highest 3.94±1.321 (Table 5), therefore SRB3 was found to be the most effective material for gamma rays shielding. The sample composition selected best for neutron shielding is SRB1 with a mean *MERC* value of 17.04± 8.70 (Table5).

5. Conclusions

The present investigation was planned with the aim of selecting novel lead free materials and studying their fast neutron and gamma shielding behavior for their further application to safeguard individuals from radiation leakage and their harmful effects. The neutron-gamma shielding behavior (NGSB) of silicon rubber matrix amalgamated with bismuth (III) oxide (Bi_2O_3) and hexagonal boron nitride (hBN) was studied using GEANT4 and Py-MLBUF in the energy range 1-10MeV based on different shielding parameters. An increase of 30% Bi_2O_3 by wt. in SRB3 increased its mass attenuation coefficient (*MAC*), equivalent atomic number (Z_{eq}) and decreased the half-value layer (*HVL*) and tenth-value layer (*TVL*) values, implicating the higher level of Bi_2O_3 in the composite sample (SRB3) improved its gamma-ray shielding capability and make it a promising gamma-shielding material. The presence of low-Z elements Hydrogen, carbon and oxygen in SRB1 improved its *MERC* value in the selected energy range and indicated SRB1 a good alternative for conventional neutron shielding materials. In general, the silicon rubber matrix amalgamated with bismuth (III) oxide (Bi_2O_3) and hexagonal boron nitride (hBN) has the potential to shielding fast neutron and gamma radiation. These multifunctional lightweight, flexible and non-toxic silicon rubber composite materials would be a favorable prospective for the advancement in nuclear radiation shielding technology specifically in the medical and nuclear research.

Acknowledgements

The authors are grateful for the open-access facilities of the GEANT4-toolkit and Py-MLBUF online platform which are used freely in this work.

References:

Agostinelli, S., J. Allison, K. Amako, J. Apostolakis, H. Araujo, P. Arce, M. Asai, et al. 2003. "GEANT4 - A Simulation Toolkit." *Nuclear Instruments and Methods in Physics Research, Section A: Accelerators, Spectrometers, Detectors and Associated Equipment* 506 (3): 250–303. https://doi.org/10.1016/S0168-9002(03)01368-8.

Ahmed, Bashir, G. B. Shah, Azhar H. Malik, Aurangzeb, and M. Rizwan. 2020. "Gamma-Ray Shielding Characteristics of Flexible Silicone Tungsten Composites." *Applied Radiation and Isotopes* 155 (June 2019): 108901. https://doi.org/10.1016/j.apradiso.2019.108901.

Al-Hadeethi, Y., and M. I. Sayyed. 2020. "A Comprehensive Study on the Effect of TeO_2 on

the Radiation Shielding Properties of TeO_2–B_2O_3–Bi_2O_3–LiF–$SrCl_2$ Glass System Using Phy-X/PSD Software." *Ceramics International* 46 (5): 6136–40. https://doi.org/10.1016/j.ceramint.2019.11.078.

Al-Hadeethi, Y., M. I. Sayyed, and Manasa Nune. 2021. "Radiation Shielding Study of WO_3–ZnO–PbO–B_2O_3 Glasses Using Geant4 and Phys-X: A Comparative Study." *Ceramics International* 47 (3): 3988–93. https://doi.org/10.1016/j.ceramint.2020.09.263.

Ambika, M. R., N. Nagaiah, V. Harish, N. K. Lokanath, M. A. Sridhar, N. M. Renukappa, and S. K. Suman. 2017. "Preparation and Characterisation of Isophthalic-Bi_2O_3 Polymer Composite Gamma Radiation Shields." *Radiation Physics and Chemistry* 130: 351–58. https://doi.org/10.1016/j.radphyschem.2016.09.022.

Amirabadi, Eskandar Asadi, Marzieh Salimi, Nima Ghaleh, Gholamreza Etaati, and and Hossien Asadi. 2013. "Study of Neutron and Gamma Radiation Protective Shield." *International Journal of Innovation and Applied Studies* 3 (4): 1079–85. http://www.issr-journals.org/ijias/abstract.php?article=IJIAS-13-156-06.

Aşkın, A. 2019. "Evaluation of the Radiation Shielding Capabilities of the $Na_2B_4O_7$–SiO_2–MoO_3-Dy_2O_3 Glass Quaternary Using Geant4 Simulation Code and Phy-X/PSD Database." *Ceramics International*, 1–7. https://doi.org/10.1016/j.ceramint.2019.12.158.

Aygün,Bünyamin. 2019. "High Alloyed New Stainless Steel Shielding Material for Gamma and FastNeutron Radiation." *Nuclear Engineering and Technology*, no. xxxx. https://doi.org/10.1016/j.net.2019.08.017.

Bagheri, Reza, Alireza Khorrami Moghaddam, and Hassan Yousefnia. 2017. "Gamma Ray Shielding Study of Barium–Bismuth–Borosilicate Glasses as Transparent Shielding Materials Using MCNP-4C Code, XCOM Program, and Available Experimental Data." *Nuclear Engineering and Technology* 49 (1): 216–23. https://doi.org/10.1016/j.net.2016.08.013.

Bashter, I. I. 1997. "Calculation of Radiation Attenuation Coefficients for Shielding Concretes." *Annals of Nuclear Energy* 24 (17): 1389–1401. https://doi.org/10.1016/S0306-4549(97)00003-0.

Bashter, I. I. 2006. "Radiation Attenuation and Nuclear Properties of High Density Concrete Made with Steel Aggregates." *Radiation Effects and Defects in Solids* 140: 37–41. https://doi.org/10.1080/10420159708216859.

Bashter, I.I, A.S. Makarious, and A.EL-Sayed Abdo. 1996. "Investigation of Hematite - Serpentine and Ilmenite- Limonite Concretes for Reactor Radiation Shielding." *Ann. Nucl. Energy* 23 (1): 65–71.

Biswas, Ripan, Hossain Sahadath, Abdus Sattar Mollah, and Md. Fazlul Huq. 2016. "Calculation of Gamma-Ray Attenuation Parameters for Locally Developed Shielding Material: Polyboron." *Journal of Radiation Research and Applied Sciences* 9 (1): 26–34. https://doi.org/10.1016/j.jrras.2015.08.005.

Chang, Le, Yan Zhang, Yujian Liu, Jun Fang, Weilin Luan, Xiangmin Yang, and Weidong Zhang. 2015. "Preparation and Characterization of Tungsten/Epoxy Composites for γ-Rays Radiation Shielding." *Nuclear Instruments and Methods in Physics Research, Section B: Beam Interactions with Materials and Atoms* 356–357: 88–93. https://doi.org/10.1016/j.nimb.2015.04.062.

Durani, L. 2009. "Update to ANSI / ANS-6.4.3-1991 for Low-Z and Compound Materials and

Review of Particle Transport Theory." *UNLV Theses, Dissertations, Professional Papers, and Capstones 43*, 69. https://doi.org/10.34917/1363554.

Durani, Luis. 2009. "Update to ANSI / ANS-6.4.3-1991 for Low-Z and Compound Materials and Review of Particle Transport Theory." *205* 43: 205. http://dx.doi.org/10.34917/1363554.

El-kameesy, Samir Yosha, Wagdy Ahmed Kansouh, Elsayed Salama, Mabrouk Kamel El-mansy, Sara Ahmed El-khateeb, and Riad Mostafa Megahid. 2017. "A Developed Material as a Nuclear Radiation Shield for Personal Wearing." *Journal of Applied Mathematics and Physics* 5: 596–605. https://doi.org/10.4236/jamp.2017.53051.

El-Khayatt, A. M. 2010. "Calculation of Fast Neutron Removal Cross-Sections for Some Compounds and Materials." *Annals of Nuclear Energy* 37 (2): 218–22. https://doi.org/10.1016/j.anucene.2009.10.022.

Erdem, Mehmet, Oktay Baykara, Mahmut Doğru, and Fatih Kuluöztürk. 2010. "A Novel Shielding Material Prepared from Solid Waste Containing Lead for Gamma Ray." *Radiation Physics and Chemistry* 79 (9): 917–22. https://doi.org/10.1016/j.radphyschem.2010.04.009.

Gallego, Eduardo, Alfredo Lorente, and Héctor René Vega-Carrillo. 2009. "Testing of a High-Density Concrete as Neutron Shielding Material." *Nuclear Technology* 168 (2): 399–404. https://doi.org/10.13182/NT09-A9216.

Harrison, Courtney, Eric Burgett, Nolan Hertel, and Eric Grulke. 2008. "Polyethylene/Boron Composites for Radiation Shielding Applications." *AIP Conference Proceedings* 969:484–91. https://doi.org/10.1063/1.2845006.

Içelli, Orhan, Kulwinder Singh Mann, Zeynel Yalçın, Salim Orak, and Vatan Karakaya. 2013. "Investigation of Shielding Properties of Some Boron Compounds Orhan." *Annals of Nuclear Energy* 55: 341–50. https://doi.org/10.1016/j.anucene.2012.12.024.

Intom, Sirilak, Ekwipoo Kalkornsurapranee, Jobish Johns, Siriprapa Kaewjaeng, Suchart Kothan, Wirapron Hongtong, Wuttichai Chaiphaksa, and Jakrapong Kaewkhao. 2020. "Mechanical and Radiation Shielding Properties of Flexible Material Based on Natural Rubber/ Bi2O3 Composites." *Radiation Physics and Chemistry* 172: 108772. https://doi.org/10.1016/j.radphyschem.2020.108772.

Mann, K.S, and S.S Mann. 2021. "Py-MLBUF: Development of an Online-Platform for Gamma-Ray Shielding Calculations and Investigations." *Annals of Nuclear Energy* 150: 107845. https://doi.org/10.1016/j.anucene.2020.107845.

Mann, K S, J Singla, V Kumar, and G S Sidhu. 2012. "Investigations of Mass Attenuation Coefficients and Exposure Buildup Factors of Some Low-Z Building Materials." *Annals of Nuclear Energy* 43: 157–66. https://doi.org/10.1016/j.anucene.2012.01.004.

Mann, K.S, Kaur,B, Sidhu, G.S, and Kumar,A., 2013. "Investigations of Some Building Materials for γ-Rays Shielding Effectiveness."*Radiation Physics and Chemistry* 87:16–25.https://doi.org/10.1016/j.radphyschem.2013.02.012.

Mirji, Rajeshwari, and Blaise Lobo. 2017. "Computation of the Mass Attenuation Coefficient of Polymeric Materials at Specific Gamma Photon Energies." *Radiation Physics and Chemistry* 135: 32–44. https://doi.org/10.1016/j.radphyschem.2017.03.001.

Mollah, A. S., G. U. Ahmad, and S. R. Husain. 1992. "Measurements of Neutron Shielding

Properties of Heavy Concretes Using a Cf-252 Source." *Nuclear Engineering and Design* 135 (3): 321–25. https://doi.org/10.1016/0029-5493(92)90199-6.

Olukotun, S. F., Kulwinder Singh Mann, S. T. Gbenu, F. I. Ibitoye, O. F. Oladejo, Amit Joshi, H. O. Tekin, et al. 2019. "Neutron-Shielding Behaviour Investigations of Some Clay-Materials." *Nuclear Engineering and Technology* 51 (5): 1444–50. https://doi.org/10.1016/j.net.2019.03.019.

Özdemir, Tonguç, and Seda Nur Yılmaz. 2018. "Mixed Radiation Shielding via 3-Layered Polydimethylsiloxane Rubber Composite Containing Hexagonal Boron Nitride, Boron (III) Oxide, Bismuth (III) Oxide for Each Layer." *Radiation Physics and Chemistry* 152 (July): 17–22. https://doi.org/10.1016/j.radphyschem.2018.07.007.

Park, Jin Ju, Sung Mo Hong, Min Ku Lee, Chang Kyu Rhee, and Won Hyuk Rhee. 2015. "Enhancement in the Microstructure and Neutron Shielding Efficiency of Sandwich Type of 6061Al-B4C Composite Material via Hot Isostatic Pressing." *Nuclear Engineering and Design* 282: 1–7. https://doi.org/10.1016/j.nucengdes.2014.10.020.

Rinard, P. 1990. "Neutron Interactions with Matter." *Los Alamos Technical Reports*, 357–77.

Rose.P.F. 1991. "ENDF/B-VISummary Document, ReportBNL-NCS-17541(ENDF-201)." In *BNL-NCS-17541*. National Nuclear Data Center,Brook haven National Laboratory,Upton,NY,USA. https://cir.nii.ac.jp/crid/1572543023985895808.bib?lang=en.

Sadawy, M. M., and R. M. El Shazly. 2019. "Nuclear Radiation Shielding Effectiveness and Corrosion Behavior of Some Steel Alloys for Nuclear Reactor Systems." *Defence Technology* 15 (4): 621–28. https://doi.org/10.1016/j.dt.2019.04.001.

Seda Nur Yılmaz, İsmail Kutlugün Akbay, Tonguç Özdemir. 2020. "A Metal-Ceramic-Rubber Composite for Hybrid Gamma and Neutron Radiation Shielding." *Radiation Physics and Chemistry*. https://doi.org/10.1016/j.radphyschem.2020.109316.

Shit, Subhas C., and Pathik Shah. 2013. "A Review on Silicone Rubber." *National Academy Science Letters* 36 (4): 355–65. https://doi.org/10.1007/s40009-013-0150-2.

Singh, Harjinder, Gurdarshan Singh Brar, Kulwinder Singh Mann, and Gurmel Singh Mudahar. 2016. "Experimental Investigation of Clay Fly Ash Bricks for Gamma-Ray Shielding." *Nuclear Engineering and Technology* 48 (5): 1230–36. https://doi.org/10.1016/j.net.2016.04.001.

Singh, Narveer, Kanwar Jit Singh, Kulwant Singh, and Harvinder Singh. 2004. "Comparative Study of Lead Borate and Bismuth Lead Borate Glass Systems as Gamma-Radiation Shielding Materials." *Nuclear Instruments and Methods in Physics Research, Section B: Beam Interactions with Materials and Atoms* 225 (3): 305–9. https://doi.org/10.1016/j.nimb.2004.05.016.

Singh, V P., and N. M. Badiger. 2012. "Comprehensive Study of Energy Absorption and Exposure Build-up Factors for Concrete Shielding in Photon Energy Range 0.015-15 MeV up to 40 Mfp Penetration Depth: Dependency of Density, Chemical Elements, Photon Energy." *International Journal of Nuclear Energy Science and Technology* 7 (1): 75–99. https://doi.org/10.1504/IJNEST.2012.046987.

Singh, V P., and N. M. Badiger. 2014. "The Gamma-Ray and Neutron Shielding Factors of Fly-Ash Brick Materials." *Journal of Radiological Protection* 34 (1): 89–101. https://doi.org/10.1088/0952-4746/34/1/89.

Singh, V P., N. M. Badiger, and A. M. El-Khayatt. 2014. "Study on γ-Ray Exposure Buildup Factors and Fast Neutron-Shielding Properties of Some Building Materials." *Radiation Effects and Defects in Solids* 169 (6): 547–59.https://doi.org/10.1080/10420150.2014.905942.

Singh, Vishwanath P., and N. M. Badiger. 2014. "Gamma Ray and Neutron Shielding Properties of Some Alloy Materials." *Annals of Nuclear Energy* 64: 301–10. https://doi.org/10.1016/j.anucene.2013.10.003.

Tellili, B., Y. Elmahroug, and C. Souga. 2014. "Calculation of Fast Neutron Removal Cross Sections for Different Lunar Soils." *Advances in Space Research* 53 (2): 348–52. https://doi.org/10.1016/j.asr.2013.10.023.

Wood, James. 1982. *Computational Methods in Reactor Shielding*. First. Oxford: Pergamon Press.

List of Tables

List of Figures

Table 1: Elemental composition of the doped silicon rubber composites

S. No	Description	Elemental Composition (%)									
		Silicon rubber	Hexagonal boron nitride	Bismuth (III) Oxide	C	H	O	Si	B	Bi	N
1	SRB1	89	0	0	0.36	0.08	0.22	0.35	-	-	-
2	SRB2	54	20	20	0.21	0.05	0.15	0.20	0.08	0.18	0.11
3	SRB3	54	10	30	0.21	0.05	0.16	0.20	0.04	0.27	0.05
4	SRB4	54	10	10	0.21	0.05	0.14	0.20	0.13	0.09	0.17

Table 2: Validation of GEANT4 using reference concretes

S.No	Material	Measured values of *ERC* (cm^{-1})		
		GEANT4 values	Experimental values	Difference (%)
1	Ordinary concrete	0.0937	0.0819	10.0
2	Magnetite	0.103	0.0949	9.0
3	Hormirad	0.143	0.1300	10.0
4	Hematite-serpentine	0.1344	0.122	10.1
5	Ilmenite-limonite	0.1291	0.124	4.0

Table 3: Mass attenuation coefficients (*MAC*) of the doped silicon rubber composites

Energy (MeV)	SRB1			SRB2			SRB3			SRB4		
	GEANT4	Py-MLBUF	Diff (%)	GEANT4	Py-MLBUF	Diff (%)	GEANT4	Py-MLBUF	Diff (%)	GEANT4	Py-MLBUF	Diff (%)
1	6.918	6.896	0.315	6.770	6.794	0.342	6.842	6.890	0.705	6.698	6.696	0.028
2	4.811	4.827	0.346	4.657	4.683	0.561	4.684	4.717	0.708	4.630	4.649	0.414
3	3.867	3.895	0.701	3.838	3.868	0.773	3.912	3.944	0.843	3.765	3.792	0.702
4	3.331	3.358	0.816	3.407	3.430	0.671	3.525	3.547	0.641	3.290	3.313	0.704
5	2.985	3.009	0.818	3.148	3.162	0.471	3.304	3.316	0.358	2.991	3.009	0.596
6	2.745	2.767	0.815	2.980	2.989	0.299	3.169	3.173	0.121	2.789	2.803	0.499
8	2.436	2.454	0.734	2.786	2.787	0.011	3.0315	3.024	0.223	2.541	2.548	0.297
10	2.251	2.267	0.689	2.689	2.687	0.083	2.978	2.969	0.313	2.400	2.405	0.206

% Diff = $MAC_{(GEANT4)}$ - $MAC_{(Py\text{-}MLBUF)}$ * 100/$MAC_{(GEANT4)}$.

Table 4: Analysis of Variance indicating the response of samples and their interaction with energy levels for *MAC* and *MERC*

Source of Variation	DF	*MAC*	*MERC*
Sample (S)	3	421.122***	11.414***
Energy Level (E)	7	627.149***	158.377***
Sample (S) x Energy (E)	21	29.111***	0.853***
Error	62	0.012	0.005

'***'0.001 (Highly Significant)

Table 5: Descriptive Statistics of samples under study

		Mean	Standard Deviation	Minimum	Maximum
MAC	SRB1	3.68	1.54	2.27	6.90
	SRB2	3.80	1.37	2.69	6.79
	SRB3	3.95	1.32	2.97	6.89
	SRB4	3.65	1.43	2.41	6.70
MERC	SRB1	17.04	8.70	9.33	36.52
	SRB2	12.31	5.55	7.36	24.72
	SRB3	11.76	5.50	6.87	24.11
	SRB4	12.83	5.55	7.86	25.16

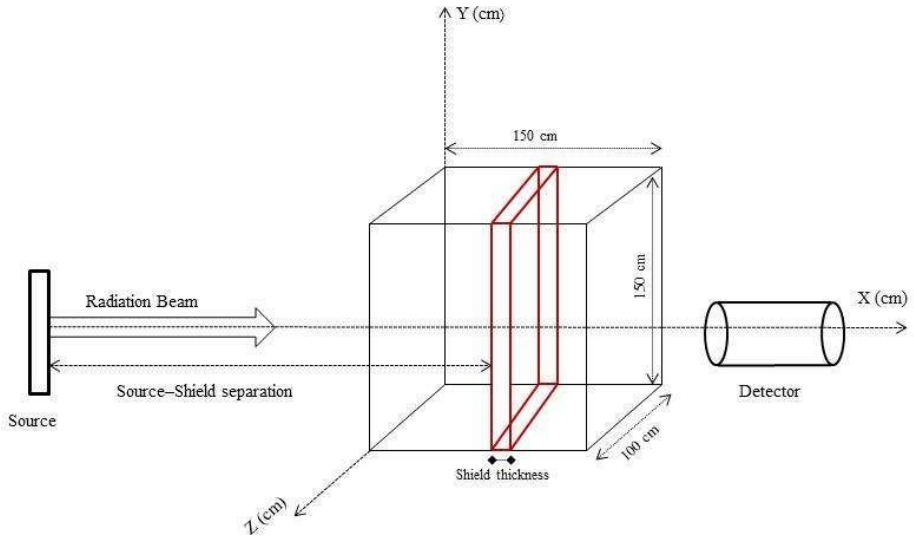
Y (cm)
150 cm
150 cm
X (cm)
Radiation Beam
Source–Shield separation
Source
Detector
100 cm
Shield thickness
Z (cm)

Fig. 1

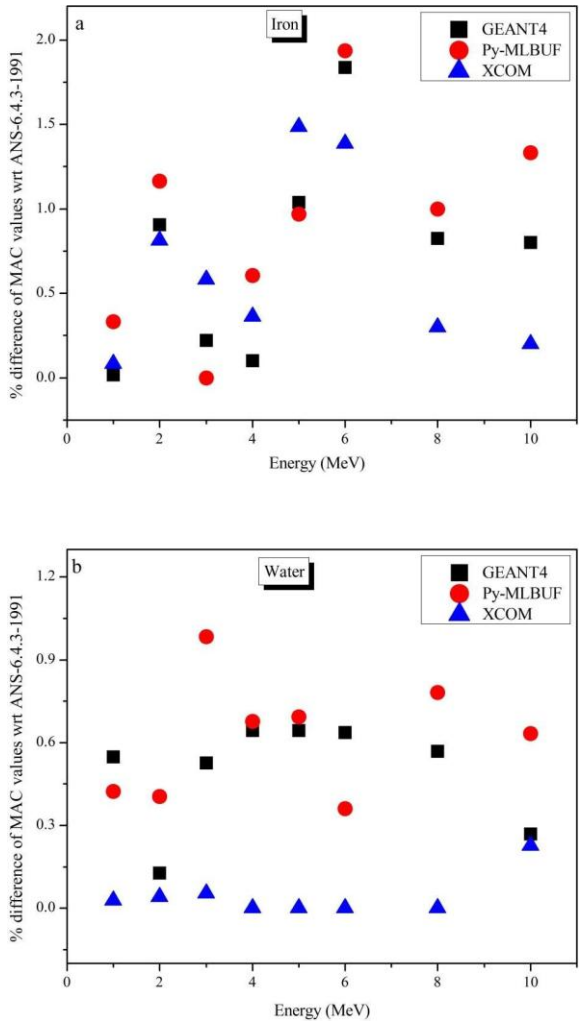
a
Iron
GEANT4
Py-MLBUF
XCOM
% difference of MAC values wrt ANS-6.4.3-1991
Energy (MeV)
b
Water
GEANT4
Py-MLBUF
XCOM
% difference of MAC values wrt ANS-6.4.3-1991
Energy (MeV)

Fig. 2

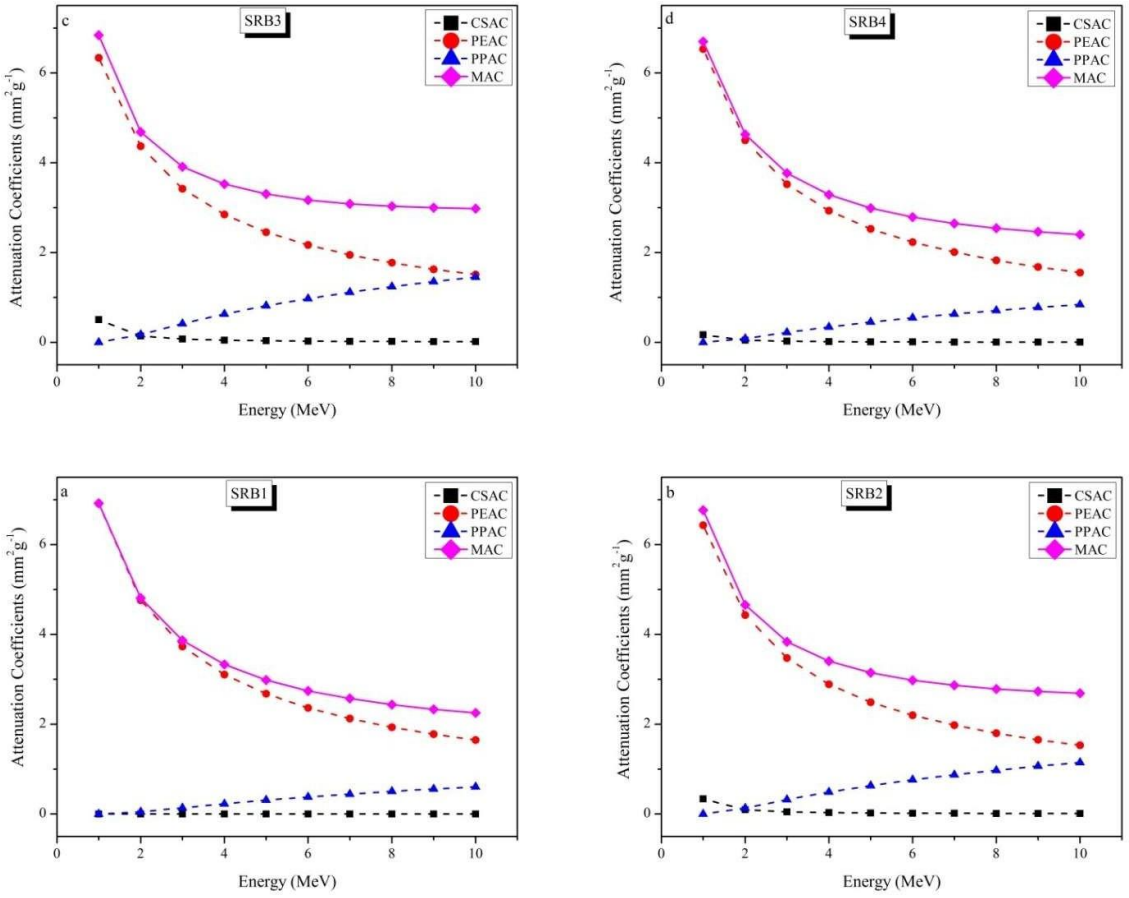
c
SRB3
CSAC
PEAC
PPAC
MAC
Attenuation Coefficients (mm^{2}g^{-1})
Energy (MeV)
d
SRB4
a
SRB1
b
SRB2

Fig. 3

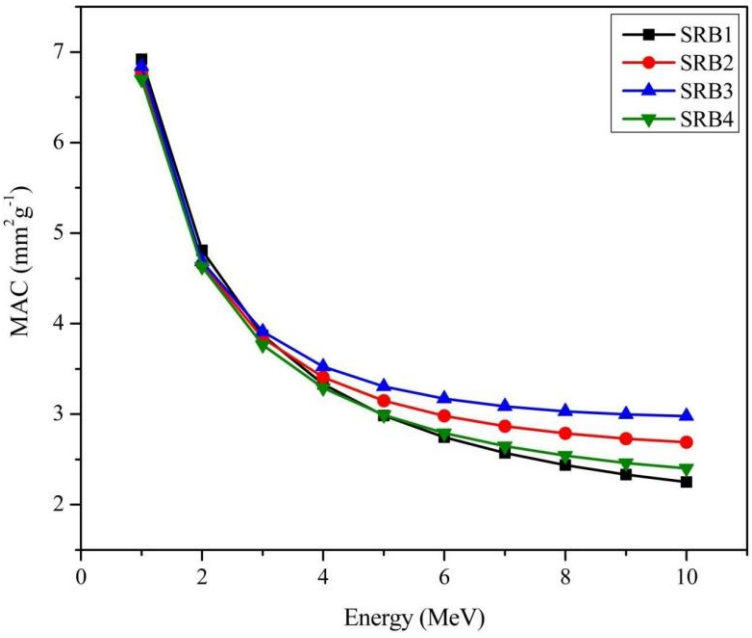
SRB1
SRB2
SRB3
SRB4
MAC (mm^{2}g^{-1})
Energy (MeV)

Fig. 4

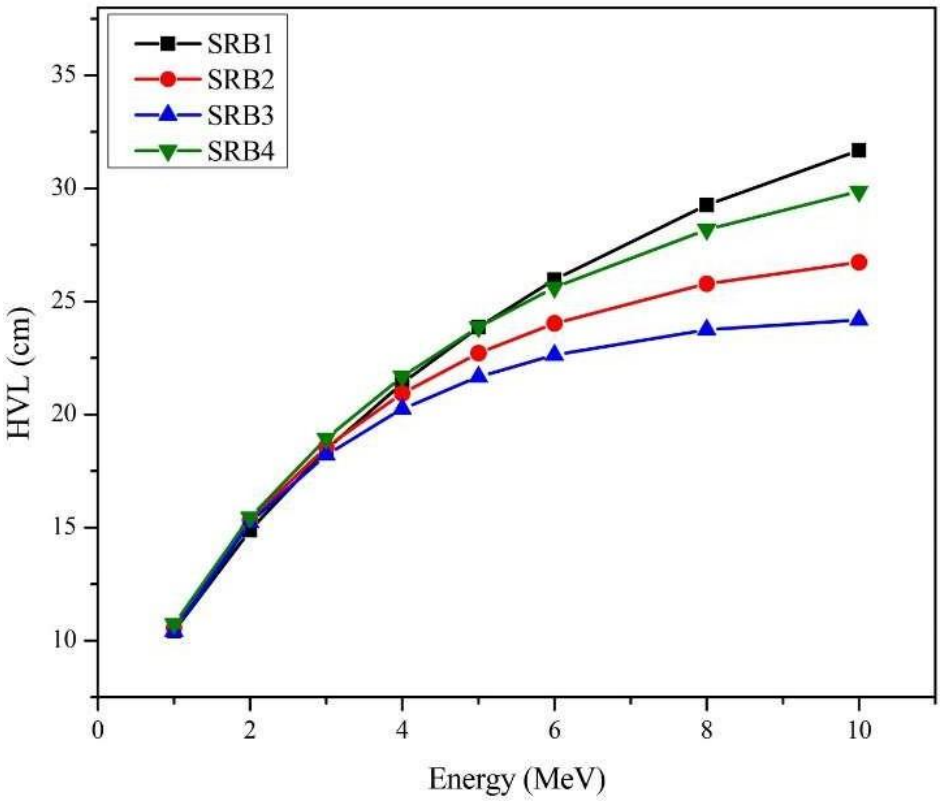
SRB1
SRB2
SRB3
SRB4
HVL (cm)
Energy (MeV)
10
15
20
25
30
35
0
2
4
6
8
10

Fig. 5

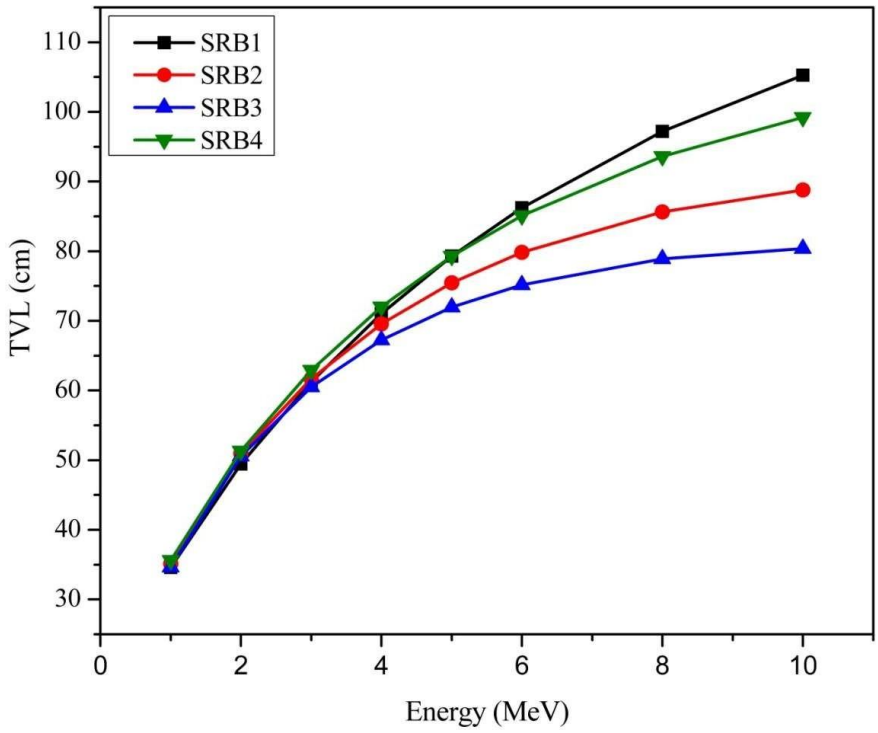
SRB1
SRB2
SRB3
SRB4
TVL (cm)
Energy (MeV)
30
40
50
60
70
80
90
100
110
0
2
4
6
8
10

Fig. 6

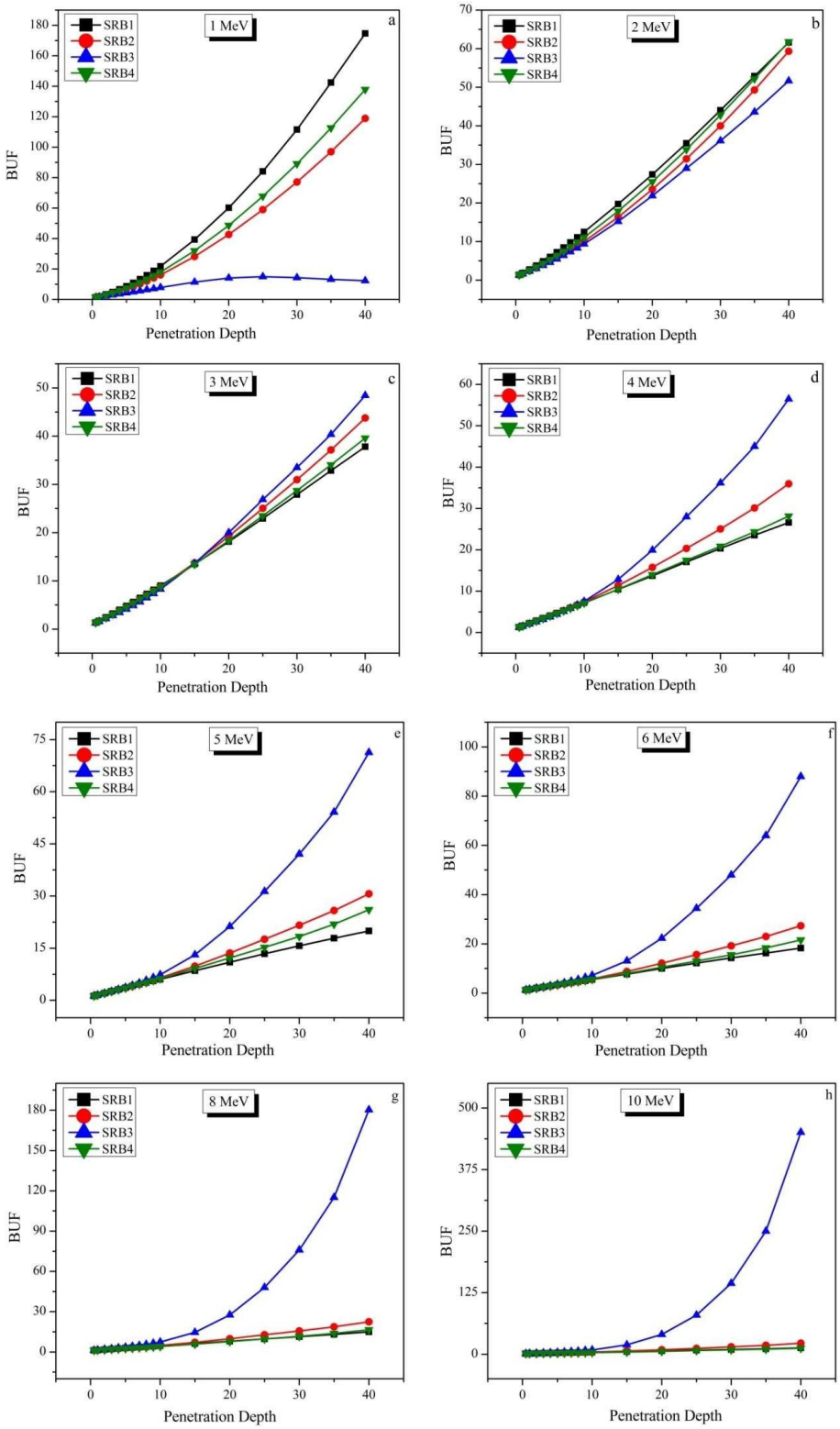
SRB1
SRB2
SRB3
SRB4
1 MeV
a
2 MeV
b
3 MeV
c
4 MeV
d
5 MeV
e
6 MeV
f
8 MeV
g
10 MeV
h
BUF
Penetration Depth

Fig. 7

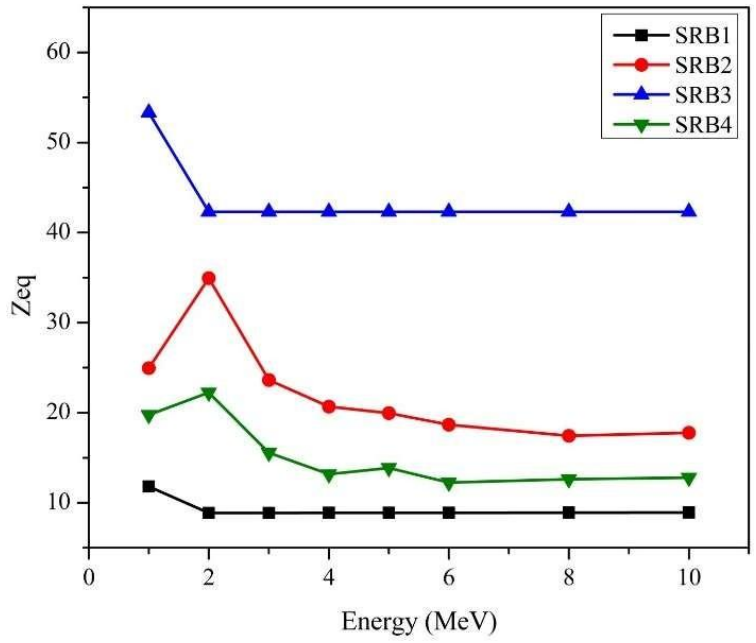
SRB1
SRB2
SRB3
SRB4
Zeq
Energy (MeV)
0
2
4
6
8
10
10
20
30
40
50
60

Fig. 8

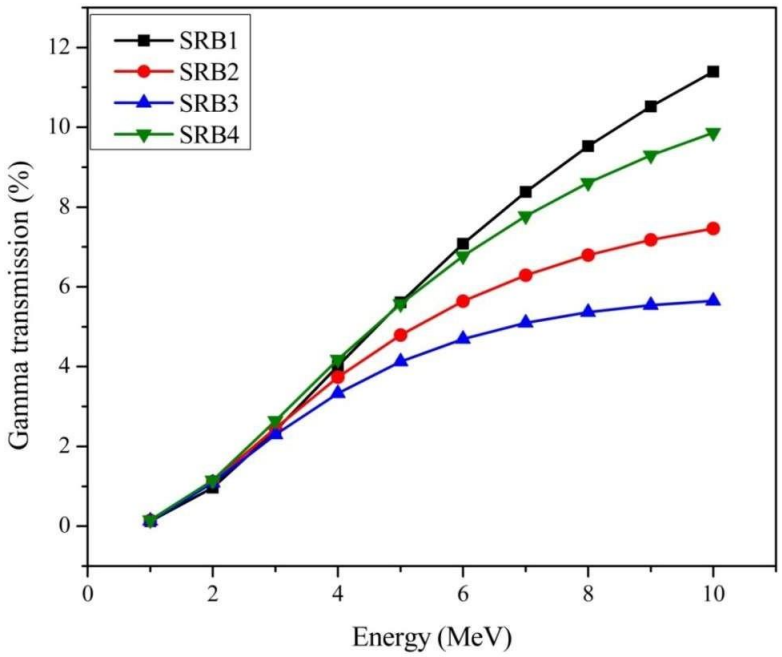
SRB1
SRB2
SRB3
SRB4
Gamma transmission (%)
Energy (MeV)
0
2
4
6
8
10
12

Fig. 9

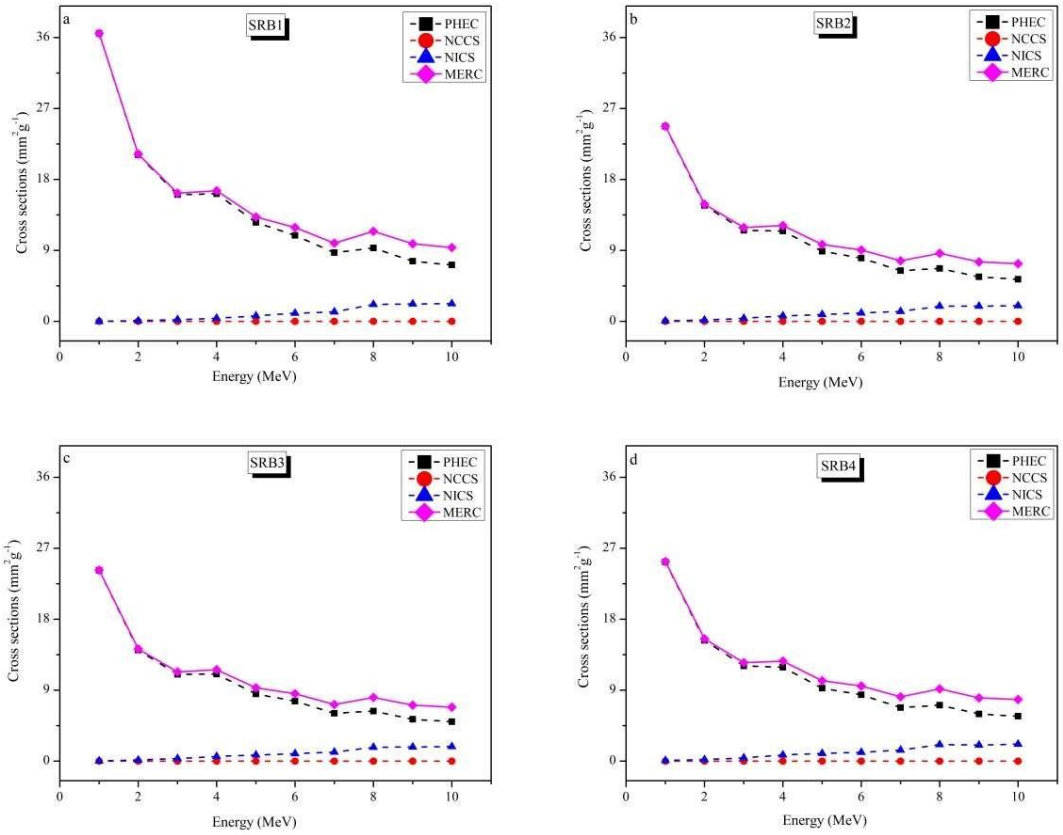
a
SRB1
b
SRB2
c
SRB3
d
SRB4
PHEC
NCCS
NICS
MERC
Cross sections (mm^{2}g^{-1})
Energy (MeV)

Fig. 10

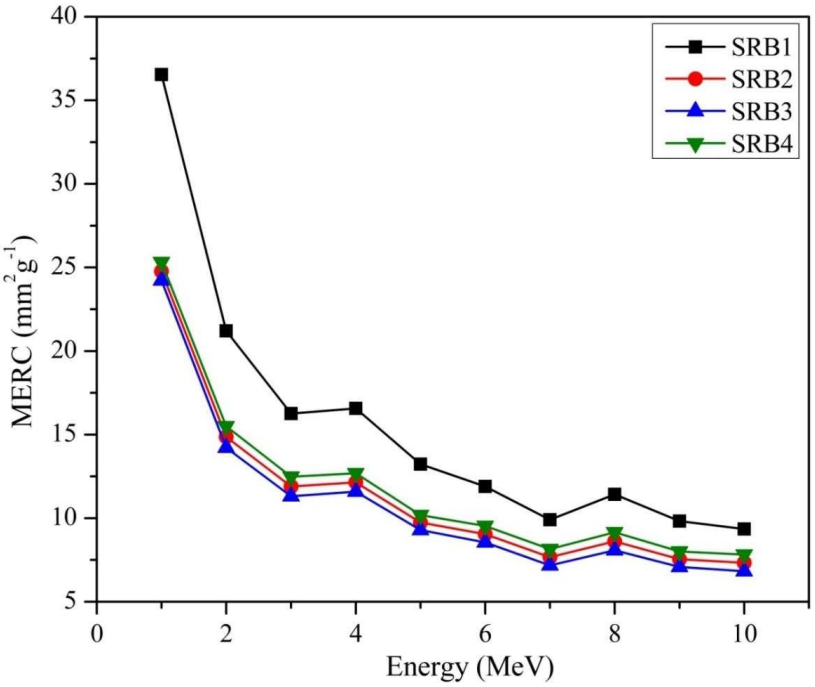
SRB1
SRB2
SRB3
SRB4
MERC (mm^{2}g^{-1})
Energy (MeV)

Fig. 11

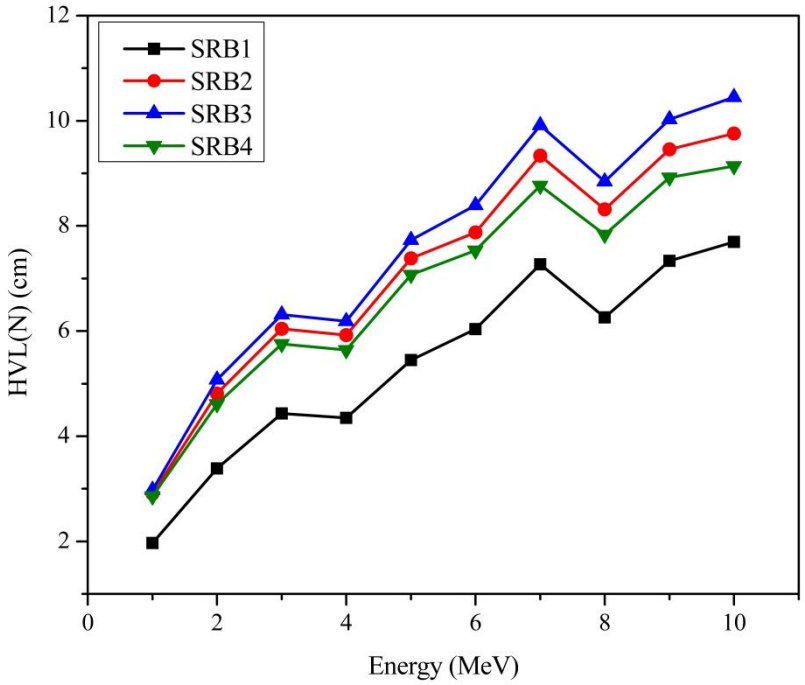
SRB1
SRB2
SRB3
SRB4
HVL(N) (cm)
Energy (MeV)
12
10
8
6
4
2
0
2
4
6
8
10

Fig. 12

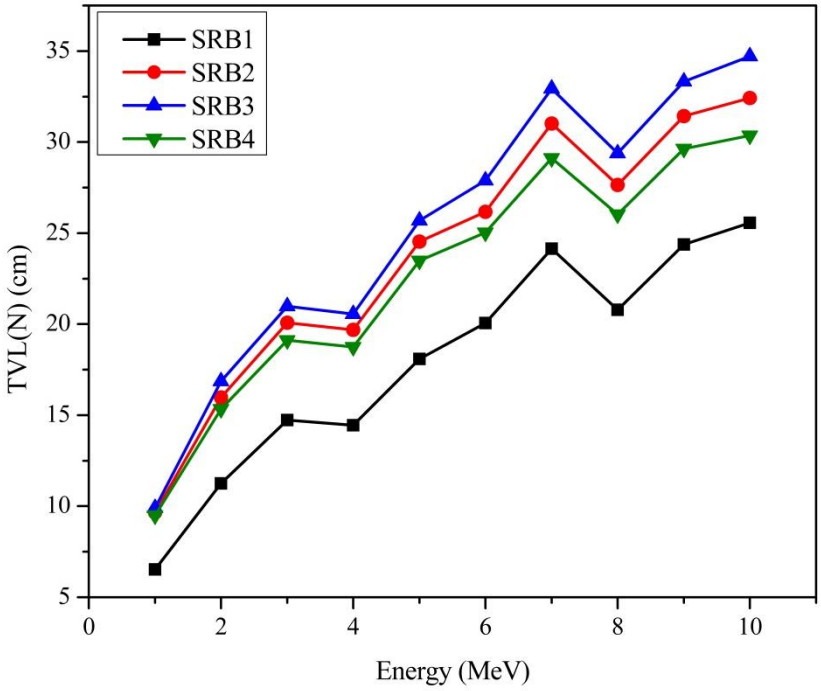
SRB1
SRB2
SRB3
SRB4
TVL(N) (cm)
Energy (MeV)
35
30
25
20
15
10
5
0
2
4
6
8
10

Fig. 13